IAC-19,A6,7,x52148

DATA FUSION APPLICATION FOR IMPROVING ORBIT DETERMINATION AND RE-ENTRY PREDICTIONS

E. Vellutini [a], G. Bianchi [b]*, C. Pardini [c], L. Anselmo [c], P. Di Lizia [d], M. Massari [d], M. Losacco [d], G. Purpura [d], F. Piergentili [e], M. Acernese [e], L. Mariani [e], S. Hadji Hossein [e], T. Pisanu [f], E. Urru [f], L. Schirru [f], F. Monaci [g], M. Peroni [g], A. Cecchini [g], G. D'Amore [a], E. Perozzi [a], L. Lama [b], C. Bortolotti [b], M. Roma [b] A. Maccaferri [b]

[a] *Italian Space Agency (ASI), via del Politecnico snc, 00133 Rome, Italy* elena.vellutini@est.asi.it, ettore.perozzi@asi.it, giuseppe.damore@asi.it
[b] *INAF - IRA, Via Piero Gobetti, 101, 40129 Bologna, Italy,* germano.bianchi@inaf.it, luca.lama@inaf.it, claudio.bortolotti@inaf.it, mauro.roma@inaf.it, andrea.maccaferri@inaf.it
[c] *ISTI-CNR, Via Giuseppe Moruzzi, 1, 56127 Pisa, Italy,* carmen.pardini@isti.cnr.it, luciano.anselmo@isti.cnr.it
[d] *Politecnico di Milano, Via Giuseppe La Masa, 34, 20156 Milano, Italy,* pierluigi.dilizia@polimi.it, mauro.massari@polimi.it, matteo.losacco@polimi.it, giovanni.purpura@polimi.it
[e] *Università La Sapienza, Via Eudossiana, 18, 00184 Roma, Italy,* fabrizio.piergentili@uniroma1.it, marco.acernese@gmail.com, mariani_lorenzo@hotmail.it, shariar.hadjihossein@gmail.com
[f] *INAF – OAC, Via della Scienza, 5, 09047 Cuccuru Angius, Selargius, Cagliari, Italy,* tpisanu@oa-cagliari.inaf.it, eurru@oa-cagliari.inaf.it, lschirru@oa-cagliari.inaf.it
[g] *Minister of Defence, Italian Air Force, Via Venti Settembre, 123/A, 00187 Roma, Italy,* fabio.monaci@aeronautica.difesa.it, moreno.peroni@aeronautica.difesa.it, andrea1.cecchini@aeronautica.difesa.it
* Corresponding Author

Abstract

Re-entry of space objects are common occurrences, which take place every day; however, risks related to these events are marginal for both people and ground infrastructures. Nevertheless, re-entry prediction of uncontrolled objects is a key capability in order to opportunely monitor the decaying of large intact space objects which, in particular cases, could pose a risk for people on the ground, such as the uncontrolled re-entry of the Chinese space station Tiangong-1 in 2018. Surveying and providing early warning of uncontrolled re-entries of spacecraft or space debris is one of the main objectives of the EUSST support framework adopted by the European Commission in 2014. This initiative is implemented by a Consortium initially formed by five European Member States (France, Germany, Italy, Spain, and United Kingdom), and expanded from 2019 with three additional EU Member States (Poland, Portugal, Romania). EUSST service provision is facilitated by EU SatCen and the three SST services, Re-entry, Collision Avoidance and Fragmentation, are provided by different member states. Italy is currently in charge of Re-entry and Fragmentation services and the current national architecture of the system is expected to evolve to improve their provision. In this perspective, an added value for the system can be given by the implementation of data fusion between radar and passive optics sensors. This technique could supply additional information about the object's dynamics (i.e. attitude motion, tumbling rate and tumbling axis orientation), which is a critical point for uncontrolled re-entry of massive objects, and it may be helpful for more refined predictions during the final phases of the descent. In addition to that, a network of sensors specifically dedicated to re-entry has the benefit of supporting the orbit determination and propagation accuracy for the whole EUSST Consortium service provision.

Keywords: Space Surveillance and Tracking; EUSST Consortium; Uncontrolled re-entries; Orbit determination; Data fusion; Re-entry predictions.

1. Introduction

The accurate re-entry prediction of uncontrolled space objects is a very challenging target because of the intrinsic physical uncertainty of the phenomenon, which is affected by several unpredictable factors such as the solar flux, the total mass and the aerodynamics of the space object. Moreover, the orbit determination process of a space object during an uncontrolled re-entry suffers from the errors and irregularities of tracking data.

Furthermore, the impact on ground of parts of a very large space object, which can also be equipped with dangerous materials, represents a very high risk for overflown population and ground infrastructures.

For this reason, European Commission decided to cope with the risks related to space objects with the Decision N. 541 of April 16th 2014 of European Parliament and of the Council, where a Framework for Space Surveillance and Tracking Support is established. As declared in the Decision, one of the specific

objectives of this Framework related to uncontrolled re-entries is "*to provide more accurate and efficient early warnings with the aim of reducing the potential risks to the safety of Union citizens and mitigating potential damage to terrestrial infrastructure*" [1].

Within this framework, five EU Member States (i.e. France, Germany, Italy, Spain and UK), with the addition from 2019 of three further EU Member States (i.e. Poland, Portugal, Romania), developed a partnership through the implementation of the EUSST Consortium. Each Member State contributes to the European Union SST capability with national assets and some of them also with a National Operations Center (NOC).

In this context, several Italian institutions cooperate, making available their specific competences for EUSST: the Italian Space Agency (ASI), acting as National Entity and operating its optical and laser sensors; the Italian Ministry of Defense (ItMoD) / Italian Air Force (ItAF), assuring SST operations through the Italian SST Operations Center (ISOC), and operating its optical and radar sensors; and the National Institute for Astrophysics (INAF), operating its optical and radar sensors.

In order to coordinate Italian capabilities, ASI, Italian MoD and INAF have created the "Coordination and Steering Committee", OCIS (*Organismo di Coordinamento e di Indirizzo*). In case of high interest events, which require a quick response as well as a deep knowledge of SST theory, OCIS can identify additional Italian entities able to give their contribution. In particular, University of Rome "La Sapienza" and CNR-ISTI have frequently been involved for their competences in orbit determination and re-entry predictions.

The Italian SST Operations Center (ISOC) is currently in charge for EUSST of the Re-entry and Fragmentation services. In particular, the Re-entry service provides information on space objects which re-enter without control in the Earth's atmosphere, fulfilling one or more of the following conditions:

- RCS larger than $1m^2$;
- Mass greater than 2.000 kg;
- Rocket bodies.

In order to improve the accuracy and to reduce the uncertainty of the re-entry predictions, data fusion techniques between radar and optical sensors have been implemented. These techniques enable the estimation of the object dynamics during uncontrolled re-entries. The knowledge of parameters such as the attitude motion, the tumbling rate and the tumbling axis orientation, allows the refinement of re-entry prediction during the final phase of the decay.

In the following paragraphs, the Italian SST ground sensor network as well as the applied software will be described, and finally both operational results of data fusion techniques and re-entry prediction improvements will be discussed.

2. Italian SST ground sensor network

For the re-entry campaigns of uncontrolled space objects ISOC can rely on a network of ground based sensors, both optical and radars. For the specific application of this paper the following sensors have been employed:

- BIRALES;
- BIRALET;
- MITO;
- SCUDO;
- SPADE;
- MLRO.

BIRALES is a bistatic radar composed of two distinct antennas, a receiving and a transmitting one with a baseline of about 580 km (see Figure 1).

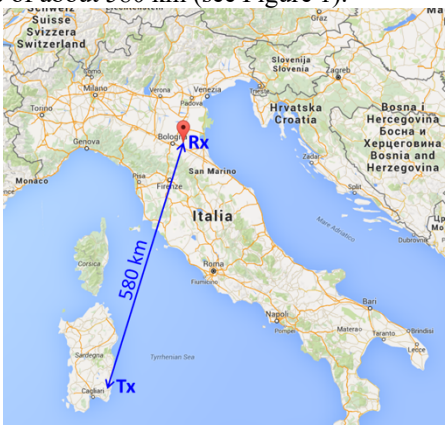

Figure 1: Tx and Rx location

The transmitting antenna is the Radio Frequency Transmitter (TRF- Figure 2) of the Italian Joint Test Range of Salto di Quirra (PISQ) in Sardinia. It consists of a powerful amplifier able to supply a maximum power of 10 kW in the bandwidth 410-415 MHz. It Is a 7 m dish completely steerable at a maximum speed of 3 deg/sec and with right hand circular polarization. It is available for operation 24 h/day. Its field of view (FoV) matches almost perfectly the receiving antenna one, with a beam of 6 deg.

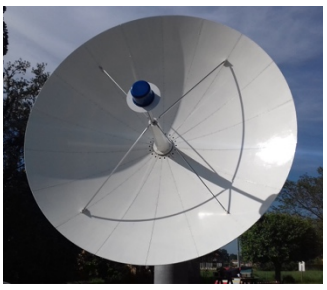

Figure 2: Radio Frequency Transmitter (TRF)

The receiving antenna is a portion of the Northern Cross Radio Telescope (Figure 3), which is currently one of the largest UHF-capable antenna in the world, being located at the Medicina Radio Astronomical Station, near Bologna, in Northern Italy.

It is owned by the University of Bologna but managed and operated by the Istituto di Radioastronomia at the Istituto Nazionale di Astrofisica (INAF-IRA). It consists of two perpendicular branches: the East-West (E/W) one is 564 m long and consists of a single cylindrical antenna with a width of 35 m, whereas the North-South (N/S) branch is made of 64 parallel antennas with a length of 23.5 m and width of 7.5 m each.

Figure 3: view of the Medicina Radio Astronomical Station. In the foreground, the Northern Cross array

At present (waiting for new upgrades to increase the field of view), the portion dedicated for the BIRALES receiving antenna is actually composed of 16 parabolic cylindrical antennas of the N/S branch (see Figure 4), with a total collecting area of about 2800 square meters. Due to the large numbers of receivers installed on the Northern Cross (4 receivers in each N/S antenna for a total of 64 receivers), the Field of View (FoV) can be populated with many independent beams.

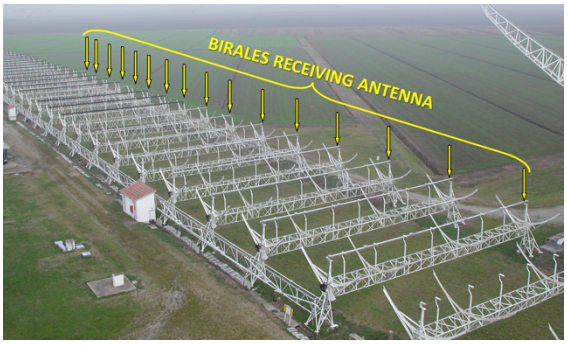

Figure 4: BIRALES receiving antenna

BIRALES works in survey mode and exploits an innovative concept based on two different systems, working at the same time:

- Multi-beam CW unmodulated
- Single-beam FMCW

The first system has the purpose of measuring the Doppler shift and the angular profiles of the target, while the second one performs the slant range measurement. For this reason, the transmitter simultaneously radiates a CW unmodulated signal centered at 410.085 MHz and a FWCM saw-tooth chirped signal with about 4 MHz bandwidth centered at 412.5 MHz. The BIRALES utilizes two different receiving chains for these two kind of signals: the echoes from the unmodulated CW are sent to a digital backend able to generate the multi-beams configuration inside the antenna FoV, whereas the chirped signals are combined into an analogue beamformer before to be processed by the ranging measurement module.

A data fusion algorithm assembles the measurements gathered simultaneously by the above systems in order to produce the TDM for the IOD. The innovative multibeam configuration of the receiver offers the possibility of estimating the track of the detected objects in the receiver field of view by analysing the beams illumination sequence. The peculiar geometrical configuration of the receiver and the complex gain pattern make this task particularly challenging, and a tailored track identification algorithm has been developed to solve the ambiguities deriving from the presence of multiple lobes of each beam inside the sensor FoV [7]. The estimated track is then coupled with the available Doppler shift and slant range measurements. Such a plethora of information offers the possibility of performing initial orbit determination (IOD) with a single passage of a resident space object inside the sensor FoV. The BIRALES system architecture in shown in the Figure 5.

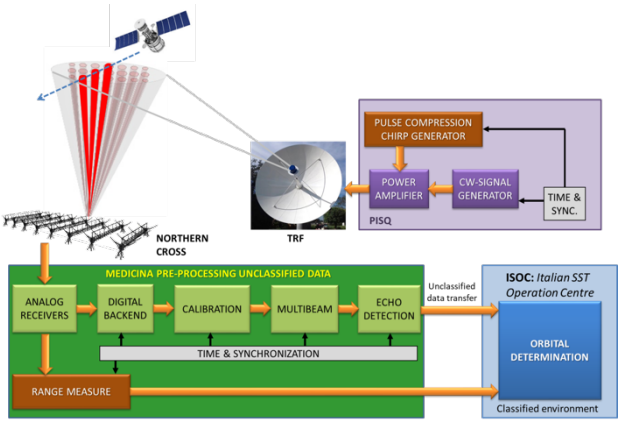

Figure 5: BIRALES system architecture

BIRALET (Bistatic Radar for Leo Tracking) is a bistatic radar operating in P band, with a 7-meter antenna and a 10 kW CW amplifier named TRF as a transmitter (Figure 2), and the SRT (Sardinia Radio Telescope), a 64 meters wheel-and-track, fully steerable parabolic antenna with a Gregorian optical configuration as a receiver ([2], [3], [4]). The SRT is designed to observe the sky with high efficiency in the frequency range between 300 MHz and 116 GHz and is able to host up to 20 remotely

controllable receivers. In order to observe the signal transmitted from the TRF and scattered by the debris, the coaxial dual-feed L-P band (0.305-0.410 GHz, 1.3-1.8 GHz) cryogenic receiver of SRT is used. BIRALET can work in beam parking or tracking mode, it has a gain of 47 dB, a 3dBbeamwidth of 0.8 degrees, a receiver noise temperature of about 20 Kelvin and a physical area of more than 3200 square meters. Now BIRALET can provide only the Doppler measurements of the observed debris and we are in a very advanced phase for upgrading it to perform pulsed signal processing and so to perform range measurement too.

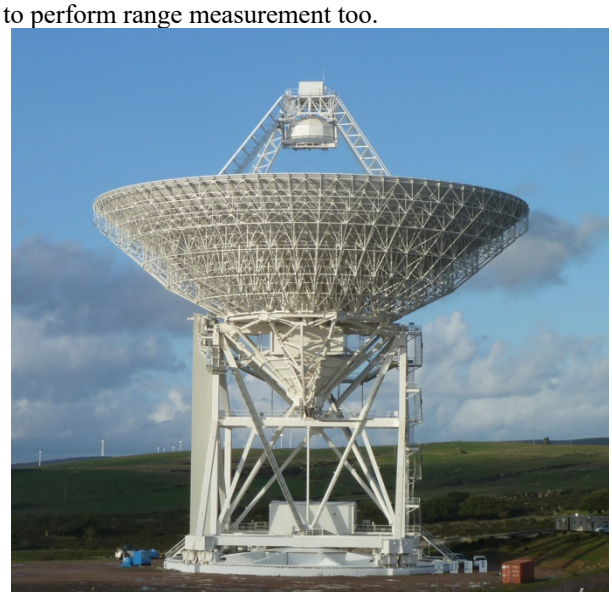

Figure 6: Sardinia Radio telescope

ASI contributes to the campaign with its laser MLRO and its telescope SPADE, both located in Matera Centre of Space Geodesy.

MLRO (Matera Lasera Ranging Observatory) currently sends data to the International Laser Ranging Services (ILRS) and the Italian Operational Centre receives and uses the overall information from ILRS, but not specifically from this laser. Jason 2, the target for this paper is a space object equipped with retro-reflector regularly tracked by MLRO.

SPADE telescope (Figure 7) has an aperture of 40 cm and a FoV of 1.38°x1.38°. It is used 100% of the time for EUSST purposes but in an experimental mode. It surveys the GEO ring 3 or 4 times a night, with about 5 seconds exposure time. It is being used mainly in surveillance mode and its data are sent to ISOC.

Figure 7. SPADE telescope

The Sapienza Scientific Observatory Network, managed by Sapienza University of Rome, has taken part in the monitoring campaign by performing optical observations. These have been used to retrieve both position angular measurements and light curves for attitude reconstruction of Tiangong-1 space station. The employed optical sensors, which are MITO, RESDOS, SCUDO and EQUO OG observatories are located in Italy and Kenya. Such a distributed geometrical configuration ensures an increased number of visible passages. All telescopes have been operated by using a sidereal tracking observation strategy.

Two optical sensors belonging to the Sapienza Scientific Optical Network [1] have been involved in the campaign.

MITO telescope (see Figure 8) has been used for the acquisition of images that have been solved in order to retrieve astrometric measurements. The acquisition of long tracklets has allowed also to extrapolate lightcurves from the images through photometric analysis. MITO is located in Rome (41.95588 N, 12.50559 E, 76 m). The optical tube mounts a 20 cm diameter mirror. It is in Schmidt-Cassegrain configuration. It has a German equatorial mount and a field of view of 3.5° x 2.5°. MITO is completely remoted.

Figure 8 MITO, located in Rome, Italy

SCUDO telescope (see Figure 9) has been used in continuous tracking mode to retrieve target objects photometric information. It is located in Collepardo, Italy. It mounts two optical tubes. One has a field of view of 2.2° x 2.2° and the other one a field of view of 1.7° x 1.1°. SCUDO is completely remoted.

Figure 9: SCUDO telescope, located in Collepardo, Italy

3. SW description

3.1 Orbit determination software for TLE optimisation

The orbit determination software for the improvement of Two-line elements through data fusion exploiting different sensors provides a solution in the Two-line elements format. The orbit determination process consists in a constrained optimisation aimed at minimising a least squares cost function constituted by the sum of the squares of the residuals.

In order for the obtained solution to be compliant with the TLE format, the SGP4 dynamical model has been employed for state propagation.

The state vector containing the variables to be estimated is constituted by Kozai – Brower mean orbital parameters:

$$\vec{x} = [i, \Omega, \mathrm{e}, \omega, \mathrm{M}, \mathrm{n}]$$

The initial guess is retrieved by a publicly available TLE, released immediately before the first processed measure.

The cost function is obtained as a weighted sum of the residuals

$$J = \frac{1}{2}\epsilon^T W \epsilon$$

where ϵ is a column vector of the *n* residuals.

In the case of angular measurements, such as those of topocentric right ascension and declination and azimuth and elevation, the *i-th* residual has been computed as the absolute angular error

$$\epsilon_i = \mathrm{acos}(\vec{\rho}_o \cdot \vec{\rho}_c)$$

where $\vec{\rho}_o$ and $\vec{\rho}_c$ are respectively the observed and computed unit vector constructed through the angular measurements.

W is a *n x n* diagonal matrix whose *i-th* diagonal term is the inverse of the variance associated to the *i-th* measure. Table 1 illustrates the standard deviations associated to each observable:

Table 1: Standard deviations associated to each observable

Observables	σ
Ra-Dec (Sapienza)	5 arcseconds
Az-El (BIRALES)	360 arcseconds
Bistatic doppler shift (BIRALES)	9 Hz
Bistatic range (BIRALES)	100 m

The software can take as input and process an arbitrary set of observations taken by different observatories.

3.2 Light curve and RADAR cross section

Even if astrometry and orbit determination maintain the most important value for the operational activities, there are a number of other information that can be obtained from observations regarding satellite attitude motion.

Light curve and radar cross section contain information on the satellite attitude motion and deserve to be analyzed since can be of paramount significance for reentering objects or malfunctioning satellites.

In this field a large experience has been achieved, during last years, from the University of Rome "La Sapienza" group and a number of software tools for determining attitude of LEO objects from light curve analysis have been implemented and tested ([6]).

Some examples of data that can be exploited to this purpose are reported in the following, from the optical side we can achieve long exposures from video and short (6 seconds) exposure from images, from radar side we can obtain analogic images lasting about six seconds.

The optical images, taken with sidereal tracking on are depicted in Figure 10. These have been obtained from Jason2 passages of 24/09/2019 from 01:35:03 to 01:37:03. Each curve last 6 seconds and have been taken 30 seconds apart each from the other. These curves have been convoluted with a 3x3 pixel matrix (for noise averaging) and have been calibrated with respect to range and atmospheric absorption.

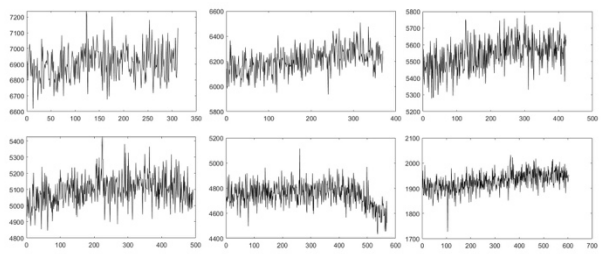

Figure 10: Jason2 short time light curves.

The sequences of images for long time light curves, have been collected by tracking the JASON2 satellite during two passages respectively on 29/09/2019 from 19:32:38 to 19:38:31 and on 30/09/2019 from 19:47:29 to 19:52:50 with exposure time ranging from 0.5 to 2 seconds. In this case the satellite is point like in the images. In this case, apart the calibration for range and atmosphere, the phase angle changing has been graphed.

Both results are visible in Figure 11 and Figure 12, these are very similar considering the similar observation geometry and the fact that the satellite is controlled.

Moreover the virtual satellite has been implemented in computer vision software and the synthetic light curve has been extracted by considering the nominal attitude of the satellite during the passage (Figure 13). It is possible to see how the virtual curve is similar to the real one, confirming the attitude of the satellite and the goodness of the realized synthetic model. In case of unknown attitude the synthetic model can be used together to optimization system developed at University of Rome "La Sapienza" to compute the inverse transformation and to identify the attitude from the lightcurve (Ref. 6).

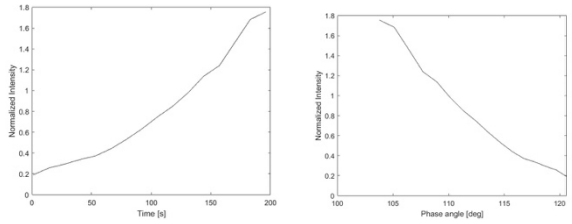

Figure 11: Jason2 29/09/2019 Long time light curves, normalized intensity with respect time anmd phase angle.

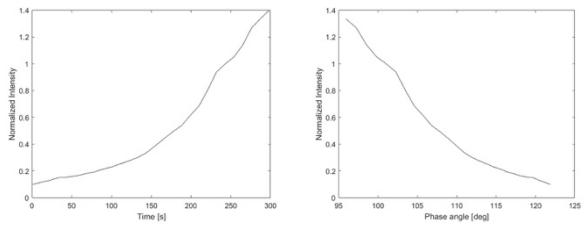

Figure 12: Jason2 30/09/2019 Long-time light curves, normalized intensity with respect time anmd phase angle.

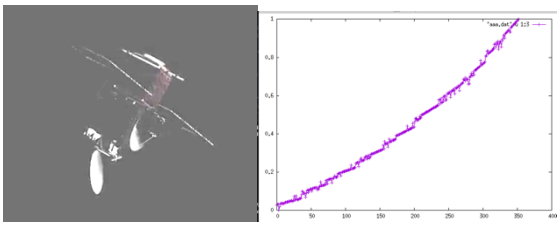

Figure 13: Jason2 virtual object and syntethic light curve of the 30/09/2019 passage

The same approach can be applied in the radar domain. Considering the variation in time of the Signal to Noise Ratio (SNR) after a radio reflection from an orbiting object, we can generate a sort of "light curve" to determine the periodic rotation or the attitude of the object. Some examples of the achieved images and extracted variations graphs are shown in Figure 1415. The figure plots the signal received by BIRALES against time during two passages of JASON2: 03/10/2019 from 12:50:07 to 12:50:15 and 04/10/2019 from 13:06:35 to 13:06:43.

From these radio curves we can derive the radar equivalent of the light curves of an optical sensor, thus giving the sense of the importance to have a network of sensors to integrate data from different source and the capability that the Italian network has to get different kind of data.

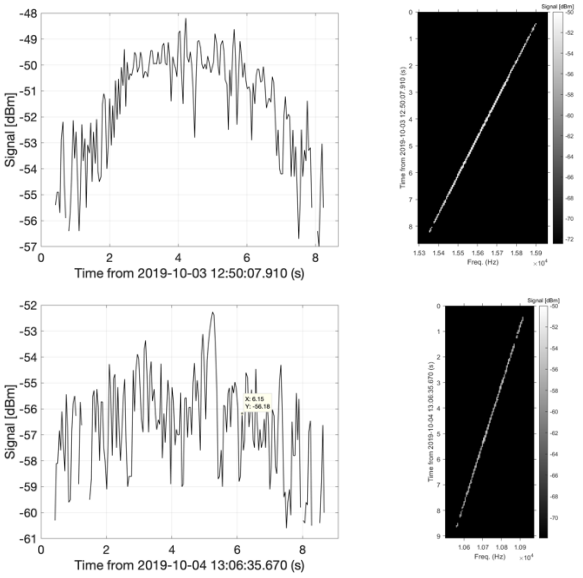

Figure 14: Signal received by BIRALES during two passages of Jason2.

4. Results

JASON 2 (catalogue number: 33105) has been selected as target of the observation campaign. Table 2 illustrates the data that has been acquired and considered for the observation campaign. Multiple sensors belonging to the different involved institutions have been exploited to increase the amount and quality of available measurements.

Table 2: number of measures of the object JASON 2 (catalogue number: 33105) acquired during the observation campaign, per day and per observatory. Set M includes bistatic range observations.

	19/09	20/09	21/09	22/09	23/09	24/09	25/09	26/09
Sapienza (RA Dec)	A=4	C=15			F=6	H=9		N=3
BIRALES (Az, El Doppler)	B=6					I=6	M=6*	
MLRO (range)			D=49			L=34		
SPADE (RA Dec)			E=1		G=1			

4.1 Orbit determination for TLE optimisation

For this study, only the optical observations produced by the Sapienza network and the radar measures produced by BIRALES have been processed. As an example, Figure 1516 illustrates the slant range measurements acquired by BIRALES during the passage of JASON 2 in the sensor FoV. For the sake of completeness, the acquired measurements have been compared with their TLE-based predictions, with a resulting root mean square deviation of 29 m.

Solution accuracy has been assessed by comparing first guess and solution residuals with respect to subsequent measures not used in the orbit determination process. First guess parameters are retrieved from the latest TLE released before the measurement.

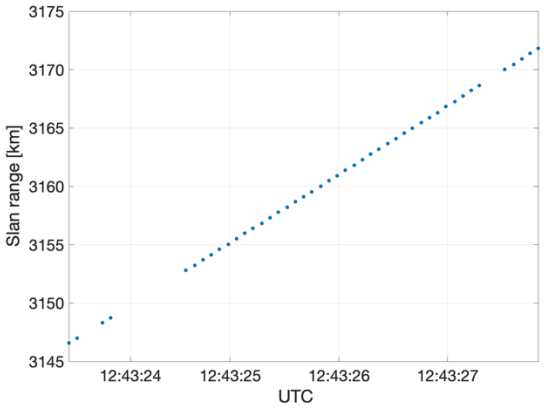

Figure 15: BIRALES slant range measurements acquired during the passage of JASON 2 in the sensor FoV on September 25, 2019.

Figure 16 compares the results obtained by combining sets A and C, without radar measures, with the results obtained by combining sets A, B and C. TLEs accuracies have been assessed by comparing the residuals with respect to measures of the H set. Both solutions are more accurate than the first guess.

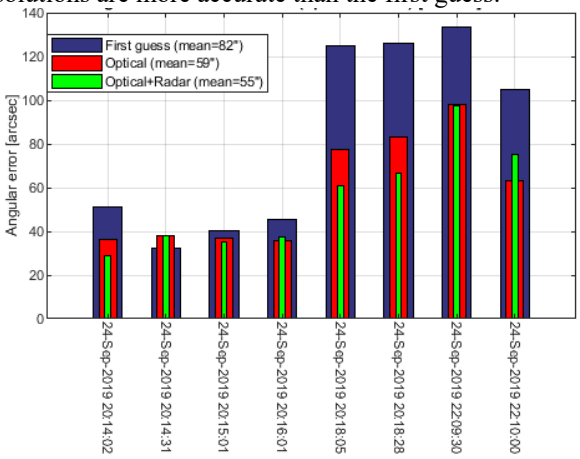

Figure 16: Results of the orbit determination for TLE improvement performed combining A-C (optical) and A-B-C (optical + radar) sets of measures. TLEs accuracies have been assessed by comparing the residuals with respect to measures of the H set.

Figure 17 compares the results obtained by combining sets F and H, without radar measures, with the results obtained by combining sets F, H and I. TLEs accuracies have been assessed by comparing the residuals with respect to measures of the N set. Both solutions are better than the first guess.

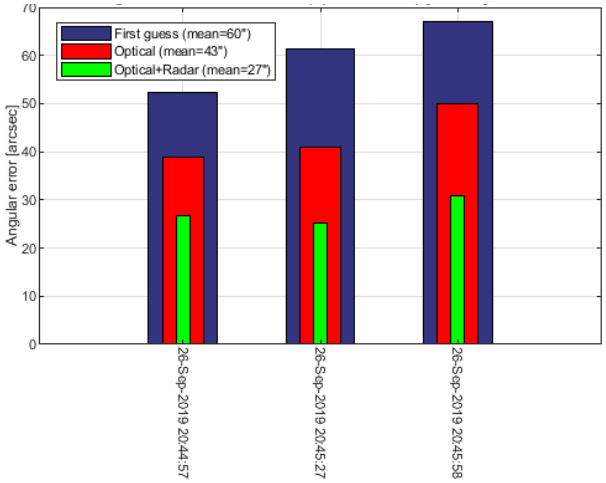

Figure 17: Results of the orbit determination for TLE improvement performed combining F-H (optical) and F-H-I (optical + radar) sets of measures. TLEs accuracies have been assessed by comparing the residuals with respect to measures of the N set.

Figure 18 compares the results obtained by combining sets F and H, without radar measures, with the results obtained by combining sets F, H and M. Set M has been processed both without and with bistatic range observations. The latter configuration provides the best improvement to the state estimate. TLEs accuracies have been assessed by comparing the residuals with respect to measures of the N set.

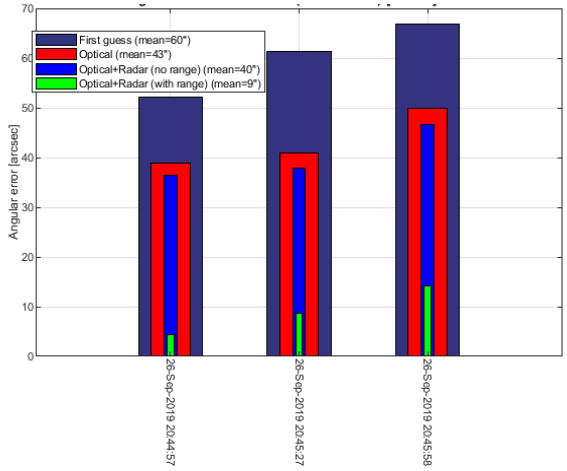

Figure 18: Results of the orbit determination for TLE improvement performed combining F-H (optical) and F-H-M (optical + radar, including range) sets of measures. TLEs accuracies have been assessed by comparing the residuals with respect to measures of the N set.

In all cases, the exclusive use of optical measurements has led to an improvement of the state estimate. By processing, together with the optical observations, radar measures, a further improvement is achieved in all test cases. Best results are obtained by including, when available, the bistatic range information.

5. RE predictions improvements

Reliable predictions of atmospheric re-entries involving uncontrolled spacecraft and orbital stages with casualty expectancy > 10^{-4} should be routinely issued as precautionary global safety measure, according to international guidelines. However, such activity is still affected by significant uncertainties, related to errors also of the best atmosphere models, to the forecasts of solar and geomagnetic activity, to the ballistic coefficient estimation and prediction, and to the accuracy and precision of the available orbit determinations ([8], [9], [10], [11], [12]). The topics covered in this paper could, at least in principle, address the last two sources of uncertainty.

The ballistic coefficient is a very sensitive parameter, depending on the re-entering object mass, size, shape, and attitude with respect to the object-atmosphere relative velocity vector. Moreover, it also depends on the composition and temperature of the object surface, on the composition of the atmosphere and, last but not least, on the aerodynamic flow regime. Depending on the cases, the underlying uncertainties on the ballistic coefficient can lead to errors in the estimation of the re-entering object residual lifetime from less than 5% to more than 50%.

Much more often than is commonly believed, the exact size, shape and mass of a re-entering intact object are not known, because the owner does not provide this information. In addition to that, also the object's attitude and its evolution are very often not known, in this case almost always unknown even for the same owner of the object. In practice, to compensate for this lack of information, the measured orbital decay of the object, over a given time span in which the space weather conditions are reasonably well known, is used in a "reverse engineering" exercise to estimate a ballistic coefficient applicable to such time interval. However, without further information, it is not possible to say how it will evolve, and the uncertainty of the re-entry prediction will inevitably grow for longer residual lifetimes.

The independent availability of several optical and radar sensors, able to observe the re-entering object, might of course be of great help in determining its general physical properties and rotational state, and data fusion from various observation techniques, as optical imaging (even at high resolution) and photometry (light-curves), laser tracking, radar cross-section estimation with mono-static and bi-static systems, high-resolution radar imaging, and so on, might certainly contribute to

refine the knowledge needed for predicting the ballistic coefficient evolution. Even though such proof of concept was not possible during the few observation runs described in this paper, this potential application of optical and radar data fusion seems the most promising in the field of uncontrolled re-entry predictions, due to the relatively large impact of the ballistic coefficient uncertainties on the estimation of the residual lifetime.

Concerning the potential benefits of optical and radar data fusion for improving the accuracy and precision of orbit determinations, it should be first of all recalled that re-entering objects are subject to a very significant drag perturbation, which is affected, as already pointed out, by quite large uncertainties. This means that even if we had a perfect and error-free orbit determination, the errors of the propagated state vector would grow rapidly in a relatively short time. Therefore, once reached a certain accuracy and precision threshold, it is much better and more useful to obtain frequent and uniformly distributed (i.e. without long temporal gaps) orbit determinations than further reducing their errors.

In LEO, but above 400 km, many analyses carried out in the past and the current experience of the Flock satellite constellation by Planet Labs, which routinely compares ranging and GPS data with CSpOC TLEs, have shown that TLE orbit determinations are affected by a root mean square position error of ~1 km, mostly along-track [13]. Below 300 km, the TLE root mean square position error might became larger, of the order of ~7-8 km, or even greater for re-entering objects [14].

Assuming nearly circular orbits at approximately 24 hours before re-entry, an along-track position error of ±1 km, corresponding to a semi-major axis error of ±100 m, would lead to an error in the residual lifetime estimation of about ±0.6%, while an along-track error of ±7.8 km, corresponding to a semi-major axis error of ±800 m, would lead to a re-entry prediction time error of nearly ±5%. The latter, more realistic for low flying objects, is certainly significant, but generally quite smaller than the error resulting from the uncertainties of ballistic coefficient, space weather forecasts and atmospheric models combined. For this reason, at such levels of accuracy and if the orbit determinations are not affected by biases, further improving the orbit determinations is not particularly advantageous compared with increasing the frequency and time coverage of them. Of course, the situation would be different in case of position errors quite larger than 10 km. In such conditions, a reliable orbit state enhancement, obtained with data fusion techniques, might be useful to improve re-entry predictions during the critical last day.

A completely different, but much less frequent situation occurs for re-entries from (highly) elliptical orbits. In such cases the TLE orbit determination uncertainties are significantly higher [15], apogee and perigee heights may be affected by considerable errors and the impact on the accuracy of re-entry predictions may be substantial. If radar measurements around the perigee and optical measurements around the apogee might be integrated to obtain a fairly refined orbit determination, the benefit for the re-entry prediction process would be appreciable. However, geometry constraints would probably preclude the conduct of similar tests with radars placed exclusively on the national territory, because geostationary transfer orbits have typically low inclinations, and the perigee of Molniya orbits remains basically locked over the southern hemisphere, thus precluding, in both cases, the visibility around the perigee from Italy.

6. Conclusions

Italy has a long-lasting background in re-entry prediction of uncontrolled space object and it is currently the provider of the Re-entry service delivered by the European EUSST consortium.

In the paper the data fusion between optical and radar measurements for the test object Jason 2 has been demonstrated to be feasible in order to improve the estimate of the state vector. By adding radar data to optical measurements, and in particular the bistatic range information, a further improvement is achieved in all test cases presented.

This technique, even if not applied to a re-entry object, appears promising in order to improve the re-entry prediction and reduce the uncertainty window when the position error of the re-entry object is large (larger than 10 km), in particular during the last crucial days of the re-entry campaign.

Acknowledgements

The research activities and operations descripted in this paper have received funding from the European Commission Framework Programme H2020 and Copernicus, “SST – Space Surveillance and Tracking” contract No. 785257-2-3SST2016 and No. 237/G/GRO/COPE/16/8935-1SST2016.

The authors gratefully acknowledge the contribution from Denis Cutajar, Alessio Magro, Josef Borg and Kristian Zarb Adami of the University of Malta, who are responsible for the development of the software back end of the BIRALES multibeam system.

References

[1] DECISION No 541/2014/EU OF THE EUROPEAN PARLIAMENT AND OF THE COUNCIL establishing a Framework for Space Surveillance and Tracking Support. L 158/227, Official Journal of European Union, 16 April 2014.

[2] G. Muntoni, L. Schirru, T. Pisanu, G. Montisci, G. Valente, F. Gaudiomonte, G. Serra, E. Urru, P. Ortu, A. Fanti, “Space debris detection in Low Earth Orbit with the Sardinia Radio Telescope”, Electronics, vol. 6, no 3, pp. 1-16, August 2017.

[3] Muntoni, G.; Schirru, L.; Montisci, G.; Pisanu, T.; Valente, G.; Ortu, P.; Concu, R.; Melis, A.; Urru, E.; Saba, A; Gaudiomonte, F.; Bianchi, G. "A Space Debris Dedicated Channel for the P-Band Receiver of the Sardinia Radio Telescope". IEEE Antennas and Propagation Magazine in press.

[4] Losacco, M.; Schirru, L. "Orbit Determination of Resident Space Objects Using the P-Band Mono-Beam Receiver of the Sardinia Radio Telescope". Appl. Sci. 2019, 9, 4092.

[5] S. Hossein, M. Acernese, G. Cialone, F. Curianò, L. Mariani, P. Marzioli., T. Cardona, V. Marini, L. Parisi, “Sapienza Space Systems and Space Surveillance Network (S5N): a high coverage infrastructure for space debris monitoring”, 69th International Astronautical Congress 2018

[6] Parisi, L., Santoni, F., Piergentili, F.,”Lightcurve inversion for attitude determination” (2018) Proceedings of the International Astronautical Congress, IAC, 2018-October.

[7] Losacco, M et al., “The Multibeam Radar Sensor Birales: Performance Assessment for Space Surveillance and Tracking”, 69th International Astronautical Congress (IAC 2018), Bremen, Germany, 1-5 Oct. 2018

[8] C. Pardini, L. Anselmo, On the accuracy of satellite reentry predictions, Adv. Space Res. 34 (2004) 1038–1043.

[9] L. Anselmo, C. Pardini, Computational methods for reentry trajectories and risk assessment, Adv. Space Res. 35 (2005) 1343–1352.

[10] C. Pardini, L. Anselmo, Re-entry predictions for uncontrolled satellites: results and challenges, In: Ouwehand L. (ed.), Proceedings of 6th IAASS Conference Safety is Not an Option, ESA SP-715, ESA Communications, European Space Agency, Noordwijk, The Netherlands, 2013.

[11] C. Pardini, L. Anselmo, Assessing the risk and the uncertainty affecting the uncontrolled re-entry of manmade space objects, J. Space Safety Eng. 5 (2018) 46–62.

[12] C. Pardini, L. Anselmo, Reentry predictions of potentially dangerous uncontrolled satellites: challenges and civil protection applications, In: Vasile M. et al. (eds), Stardust Final Conference: Advances in Asteroids and Space Debris Engineering and Science, Springer International Publishing AG, pp. 265–282, 2018.

[13] K. Riesing, K. Cahoy, Orbit determination from two line element sets of ISS-deployed cubesats, 29th Annual AIAA/USU Conference on Small Satellites, 2015

[14] D.A. Vallado, B. Bastida Virgili, T. Flohrer, Improved SSA through orbit determination of two-line element sets, Proc. 6th European Conference on Space Debris, ESA SP-723, European Space Agency, Darmstadt, Germany, 2013.

[15] C. Früh, T. Schildknecht, Accuracy of two-line-element data for geostationary and high-eccentricity orbits, J. Guid. Control Dyn. 35 (2012) 1483–1491.